DOI: https://doi.org/10.57233/ijsgs.v10i1.611 ISSNp: 2488-9229; ISSNe: 3027-1118

IJSGS FUGUSAU VOL10 (1) WEBSITE: https://fugus-

INTERNATIONAL JOURNAL OF SCIENCE FOR GLOBAL SUSTAINABILITY

(A PUBLICATION OF FACULTY OF SCIENCE, FEDERAL UNIVERSITY GUSAU)

Enhancing Thermophoresis Effect on Time-Dependent Magnetohydrodynamics (MHD) Oscillatory Boundary Layer Flow Occupied with Nanoparticles

Halima Usman[1*], Aminu Muhammad[1,2] and Emmanuel Omokhuale[2]

[1*]Department of Mathematics, Faculty of Physical and Computing Sciences, Usmanu Danfodiyo University, P.M.B. 2346, Sokoto, Nigeria

[2]Department of Mathematics, Faculty of Science, Federal University Gusau, P. M. B. 1001, Zamfara State, Nigeria

***Corresponding Author's Email:** hhalimausman@yahoo.com

Received on: January, 2024 **Revised and Accepted on:** March 2024 **Published on:** March 2024

ABSTRACT

This paper describes the impact of thermophoresis parameter on the heat and mass transfer of a nanofluid flow past a semi-infinite flat plate in a rotating system, considering unsteady magneto hydrodynamics (MHD) and free convection. A significant contribution of this research is the derivation of closed-form analytic solutions for the momentum, energy and concentration equations. The research explores the effect of various parameters on the velocity, temperature, and concentration distribution of the nanofluid, as well as the skin friction coefficient, Nusselt number, and Sherwood number. Different types of nanoparticles are considered, and the findings are presented through graphs and tables. This model has practical applications in the fields of data storage, biomedicine, and resonance imaging. In addition, graphical comparison between Narayana and Venkateswarlu (2016) with the present work demonstrate an excellent relationship, thereby affirming the accuracy and precision of this present analysis.

Keywords: Thermophoresis effect, Nanoparticles, Magnetohydrodynamics (MHD), Porous Medium, Heat Generation/Absorption.

1.0 INTRODUCTION

Over the years, research activities into small particle (such as dust or aerosol) deposition owing to thermophoresis in the presence of substantial temperature gradients has grown in importance in many technical applications. Many technical applications use thermophoresis to remove small particles from gas streams, determine exhaust gas particle trajectories from combustion devices and examine particulate material deposition on turbine blades. Thermal precipitators, which are sometimes more successful than electrostatic precipitators in removing submicron-sized particles from gas streams, also use thermophoresis. Because industrial air pollution is a worldwide concern, this phenomenon can be used to reduce air pollution by eliminating tiny particles from gas streams and other flue gases. This phenomenon frequently makes substantial contributions to atmospheric and environmental sciences, as well as aerosol research and technology. In high temperature aerosol flow reactors, thermophoresis can also be utilized to produce fine ceramic powders such as aluminum nitride (Alam 2016). Several works on thermophoresis and Brownian motion have been published in light of their diverse uses. Jha and Samaila (2022) explored the mass and heat transfer flow of an electrically conducting and incompressible fluid along an inclined permeable plate in the presence of thermophoresis and suction/injection effects. Sharma *et al.* (2023) investigated the effects of thermophoresis and Brownian motion on hydromagnetic mixed convective flow across an inclined moving plate, as well as thermal radiation and chemical reaction impacts. Waini *et al.* (2023) examined the MHD radiative flow and thermal properties of a non-Newtonian Reiner-Philippoff nanofluid with Brownian and thermophoresis diffusion effects in a non-Newtonian Reiner-Philippoff nanofluid. Jalili *et al.* (2023) examined the problem of a transient rotating inclined plate for the flow of three dimensional thin film nano materials under the effect of Brownian motion using two analytical methodologies. Suma *et al.* (2023) discussed the implication of Brownian motion and thermophoresis impacts on a hydromagnetic heat and mass transfer with Jeffrey fluid flow affected by nanoparticle along an upstanding plate. Khan and Pop (2010) explored the steady two-dimensional laminar nano fluid flow and heat transfer caused by stretching a sheet, as well as Brownian motion and thermophoresis. After translating the governing PDEs into a collection of ODEs, the governing equations were numerically solved. Mustafa *et al.* (2010) investigated the flow of incompressible nanofluids, heat and mass transfer in a channel with Brownian motion and thermophoresis effects. The governing equations were transformed from PDEs to ODEs using appropriate similarity transformations and solved numerically with RK4 and analytically with HAM. Chamkha *et al.* (2011) addressed the problem of boundary-layer nanofluid flow, heat and mass transfer in the presence of a magnetic field, heat source/sink, thermophoresis, Brownian motion, and suction or injection effects on a dynamic porous media. The governing equations were converted into an ODE system and quantitatively solved using the finite difference method (FDM).

Understanding the effect of heat generation or absorption on fluid flow is very key in many technological and physical problems of exothermic or endothermic fluid response nowadays, and these effects are crucial in monitoring the heat transmission (Gambo *et al*. 2021). Several scholars have analyzed the effects of heat-generating/absorbing fluid on various flow regimes. In view of these advantages, Ojemeri *et al.* (2024) recently presented a steady state solution of an Arrhenius-controlled fluid affected by heat generation/absorption flowing across a superhydrophobic microchannel that is heated alternatively. In addition, Ojemeri and Onwubuya (2023) describe the analysis of steady mixed convection flow of Arrhenius-controlled chemical reaction and an exothermic fluid along an isothermally heated superhydrophobic microchannel due to heat source/sink. In another paper, Ojemeri and Hamza (2022) presented a theoretical investigation of a chemically reactive fluid in a MHD natural convection flow blended with heat source and sink effects employing homotopy perturbation approach. They concluded that raising the viscous heating parameter significantly encourage the fluid motion and the volume flow rate respectively. Oni and Jha (2019) investigated the effects of a heat source and sink fluid on natural convection confined to an upstanding annulus with time-periodic heating boundary conditions. They discovered that heat generation and absorption parameters affect velocity distribution, periodic temperature profile, Nusselt number, and frictional force at the cylinder walls, respectively. Gambo and Gambo (2020) extensively scrutinized the effects of fully developed natural convective flow of heat generating/absorbing fluid in an open-ended vertical concentric annulus with a magnetic field effect. Their findings show that by carefully selecting appropriate values for the heat generation or absorption parameter and the Hartmann number, they may be used to control the temperature and velocity profiles. Zhao *et al*. (2021) highlighted the effects of heat generation/absorption, dissipation, radiative heat flux and joule heating on the mixed convective entropy optimized nanomaterial MHD flow of Ree-Eyring fluid formed by two rotating disks. The consequences of thermal radiation, a heat source, and an induced magnetic field on the natural convective flow of a couple stress fluid in a flux-isothermal vertical channel have been evaluated by Hasan *et al*. (2020) using the method of an indeterminate coefficient. Parthiban and Pasad (2023) outlined a theoretical investigation of radiative-convection effects on MHD fluid flow in a heated square enclosure having a non-Darcy square cavity in the coexistence of the Hall effect and the heat source or sink.

Numerous works has been carried out to investigate the performance of free convection flow submerged in a porous medium along various flow channels under different physical settings. To this end, Bordoloi *et al.* (2023) outlined an analytical solution for two-dimensional steady, viscous, incompressible hydromagnetic free convective flow across a uniformly stretching upstanding porous plate submerged in a porous medium in the coexistence of Soret effect and chemical reaction. Ajibade *et al.* (2023) highlighted the effects viscous and Darcy dissipation in a steady fully developed free convection flow in a composite channel partially saturated with porous medium due heat generation using homotopy perturbation approach. Natural convection in porous media in a highly nonlinear metaphysical engineering applications was demonstrated by Kadeethum *et al.* (2022). The MHD convection flow of Casson fluid in micro-channels including porous material was discussed by Gireesha and Sindhu (2020). When Alam *et al*. (2021) used network simulation method solutions to analyze time-dependent hydro-magnetic radiative fluid flow over an inclined porous plate with heat and mass permeability, they found that the fluid momentum tended to rise or fall gradually towards the plate and then diminish or grow slowly away from the plate. The temperature of the fluid has been reported to exhibit the same tendency. Abbas *et al.* (2022) examined various industrial operations involve frequent heating and cooling of electrical systems through porous medium. Alvarez *et al.* (2022) study a stationary double diffusive natural convection problem in porous medium. Khalil *et al*. (2022) explored heat transfer by natural convection within the trapezoidal enclosure.

Recent trends in nanotechnology have made it much easier to create nanoparticles or nanostructures with higher thermophysical properties than their bulk counterparts utilising nuclear or molecular processes. Salah *et al.* (2023) developed nanofluids by dispersing nanoparticles in a base fluid such as water, oil, or ethylene glycol, to name a few. The study of nanofluids has seen a rise in research activity throughout the years. Choi (1995) introduced the first nanofluid theory. Several researchers have studied heat and mass transfer in MHD nanofluid flows. Usman and Sanusi (2023) have explored the effects of non-Newtonian nanofluid flows across a semi-infinite flat plate immersed in a porous medium on heat radiation, Soret and pressure terms. They took into account the surface temperature and concentration, which are oscillatory in nature due to the presence of various types of nanoparticles. Gbadeyan *et al.* (2020) investigated the effect of changing thermal conductivity and viscosity on non-Newtonian nanofluid flow when convective heating and velocity slip were present. Satya *et al.* (2016) studied heat and mass transfer on MHD nanofluid flow past vertical porous plate in a rotating system effect, taking into account the influence of chemical reaction and heat source on MHD and eventually determining that the Copper nanoparticles proved to have the

DOI: https://doi.org/10.57233/ijsgs.v10i1.611 ISSNp: 2488-9229; ISSNe: 3027-1118

maximum cooling recital compared to Alumina and Titanium oxide. Prasad *et al.* (2018) conducted a rigorous examination of the heat and mass transfer analysis for the MHD flow of nanofluid with radiation absorptions. They investigated the effects of diffusion, thermodynamics, and chemical reactions on the free convection heat and mass transfer flow of nanofluid over a vertical plate embedded in a porous medium in the presence of radiation absorption and a heat source under fluctuating boundary conditions. They discovered that increasing the Dufour number and radiation absorption parameter leads to an increase in thermal boundary layer thickness, while decreasing the species concentration with increasing valence. Narayana and Venkateswarlu (2016) investigated the implications of chemical reaction and heat source effects on unsteady MHD free convection heat and mass transfer in a rotating system with a nanofluid flow past a semi-infinite flat plate. Mabood and Usman (2019) investigated the influence of numerous slips on MHD nanofluid boundary layer flow with heat and mass transfer in a Darcy porous media. They investigated the effect of Darcy number and magnetic field parameters in their work and discovered that increasing the Darcy number and magnetic field parameter leads to increased friction and heat transfer rate. Chu *et al*. (2020) investigated the nonlinear thermal radiation and heat sink/source of a bidirectional periodically moving surface driven flow in a rate type nanofluid containing a gyrotactic microbe. Recently, Saleem *et al.* (2024) research on significance of hafnium nanoparticles in hydromagnetic non-Newtonian fluid-particle suspension model through divergent channel with uniform heat source. Khedher *et al.* (2024) provided novel current research to control thermal and magnetic boundary layer in the presence of viscous dissipation and induced electromagnetic field.

The main purpose of this research is to modify the work of Narayana and Venkateswarlu (2016) by evaluating the Unsteady MHD free convective flow of Thermophoresis impact through porous medium with effect of heat source/sink. The resultant nonlinear equations of velocity, temperature and concentration, which govern the fluid flow, heat and mass transfer are solved by using perturbation technique. The effects of various physical parameters on fluid velocity, temperature, concentration, skin friction coefficient, Nusselt number and Sherwood number at the plates are derived, discussed and shown through graphs. Thermophoretic depositions are significant in aerosol flow reactors because it is desirable to reduce deposition during the operation in order to maximize product yield. Hence, the motivation for this present study.

2.0 MATHEMATICAL FORMULATION OF THE FLOW PROBLEMME

Consider an unsteady MHD nanofluid flow past a semi-infinite vertical permeable plate in a rotating system with chemical reaction, thermal diffusion and thermal radiation in the presence of a uniform transverse magnetic field. It is assumed that there is no applied voltage which implies the absence of an electric field. The flow is assumed to be in the x - direction which is taken along the plate in the upward direction, the Y –axis is normal to it and the z axis along the width of the plate. Also it is assumed that the whole system is rotated with a constant vector Ω about z –axis. Due to semi-infinite plate surface assumption, the flow variables are functions of z and time t only. Following Narayana and Venkateswarlu (2016) and assuming that the fluid is controlled by thermophoresis and Brownian motion effects, the governing equations of this model can be written in dimensional form as follow:

Continuity Equation:

$$\frac{\partial w'}{\partial z'} = 0 \tag{2.1}$$

Momentum Equation:

$$\frac{\partial u'}{\partial t'} + w'\frac{\partial u'}{\partial z'} - 2\Omega u' = \frac{1}{\rho_{nf}}\left\{\mu_{nf}\frac{\partial^2 u'}{\partial z'^2} + (\rho\beta)_{nf} g\beta(T' - T'_\infty) - \frac{v_f u'}{k} - \frac{\sigma\beta_0^2 u'}{\rho}\right\} \tag{2.2}$$

$$\frac{\partial v'}{\partial t'} + w'\frac{\partial v'}{\partial z'} + 2\Omega u' = \frac{1}{\rho_{nf}}\left\{\mu_{nf}\frac{\partial^2 v'}{\partial z'^2} - \frac{v_f v'}{k} - \frac{\sigma\beta_0^2 v'}{\rho}\right\} \tag{2.3}$$

Energy Equation:

$$\frac{\partial T'}{\partial t'} + w'\frac{\partial T'}{\partial z'} = \alpha_{nf}\frac{\partial^2 T'}{\partial y'^2} - \frac{Q_H}{(\rho C_P)_{nf}}(T' - T'_\infty) + \frac{D_T}{T_\infty}\left[\left(\frac{\partial T'}{\partial z'}\right)^2\right] \tag{2.4}$$

Mass Concentration /Diffusion Equation:

$$\frac{\partial c'}{\partial t'} + w'\frac{\partial c'}{\partial z'} = D_m\frac{\partial^2 c'}{\partial z'^2} + D_L\frac{\partial^2 T'}{\partial z'^2} - R_m(C' - C'_\infty) \tag{2.5}$$

The appropriate boundary conditions are:

$$u'(z't') = 0, v'(z't') = 0, T(z't') = 0,\ C(z't') = 0\ \ for\ t' \le 0$$
$$u'(z't') = 1 + \frac{\varepsilon}{2}(e^{int} + e^{-int}), v(0,t) = 0, T(0,t') = 1,\ C(0,t') = 1$$
$$u'(\infty,t') \to 0, v'(\infty,t') \to 0, T'(\infty,t') \to 0,\ C'(z't') \to 0\ for\ t \ge 0 \tag{2.6}$$

The properties of nanofluids are defined as follows:

$$p_{nf} = (1 - \emptyset)p_f + \emptyset p_s,\ (\rho C_p)_{nf} = (1 - \emptyset)\ \ (\rho C_p)_f + \emptyset(\rho C_p)_s$$

DOI: https://doi.org/10.57233/ijsgs.v10i1.611 ISSNp: 2488-9229; ISSNe: 3027-1118
IJSGS FUGUSAU VOL10 (1) WEBSITE: https://fugus-

$(\rho\beta)_{nf} = (1-\emptyset)\ \ (\rho\beta)_f + \emptyset(\rho\beta)_s,\ \mu_{nf} = \frac{\mu_f}{(1-\emptyset)^{2.5}},\ \alpha_{nf} = \frac{K_{nf}}{(\rho C_p)_{nf}}$

$K_{nf} = K_f\left\{\frac{K_s+2K_f-2\emptyset(K_f-K_s)}{K_s+2K_f+2\emptyset(K_f-K_s)}\right\}$ (2.7)

Introducing the following non dimensional quantities are:

$u = \frac{u'}{U_0}, v = \frac{v'}{U_0}, z = \frac{U_0}{vf}z', t = \left(\frac{U_0^2}{V_f}\right)t', n = \left(\frac{V_f}{U_0^2}\right)n', R = \frac{2\Omega vf}{U^2}, S = \frac{w_0}{U_0}, Sc = \frac{v}{D_B}, Sr = \frac{D_T(T_w-T_\infty)}{(C_w-C_\infty)T_\infty}$, $T = \frac{(T-T_\infty)}{(T_w-T_\infty)}, C = \frac{(C-C_\infty)}{(C_w-C_\infty)}, Nt = \frac{(\rho c)_p D_T(T_w-T_\infty)}{(\rho c)_f T_\infty v}$, (2.8)

Inserting eqn (2.8) into eqns (2.2-2.6), we have the following dimensionless equations

$A_3\left\{\frac{\partial u}{\partial t} - S\frac{\partial u}{\partial z} - Rv\right\} = \frac{1}{A_1}\frac{\partial^2 u}{\partial z^2} + A_4 T - \left(M + \frac{1}{K}\right)u$ (2.9)

$A_3\left\{\frac{\partial v}{\partial t} - S\frac{\partial v}{\partial z} + Ru\right\} = \frac{1}{A_1}\frac{\partial^2 v}{\partial z^2} - \left(M + \frac{1}{K}\right)v$ (2.10)

$A_5\left\{\frac{\partial T}{\partial t} - S\frac{\partial T}{\partial z}\right\} = \frac{1}{Pr}\left\{A_2\frac{\partial^2 T}{\partial z^2} - QT\right\} + Nt\left[\frac{\partial T}{\partial z}\right]^2$ (2.11)

$\frac{\partial C}{\partial t} - S\frac{\partial C}{\partial z} = \frac{1}{Sc}\frac{\partial^2 C}{\partial z^2} + Sr\frac{\partial^2 T}{\partial z^2} - KrC$ (2.12)

Where $A_1 = (1-\emptyset)^{2.5},\ A_2 = \frac{K_{nf}}{K_f} + \frac{4F}{3}, A_3 = 1 - \emptyset + \emptyset\left(\frac{p_s}{p_f}\right), A_4 = 1 - \emptyset + \emptyset(\rho\beta)_s/(\rho\beta)_f$

$A_5 = 1 - \emptyset + \emptyset\left(\rho C_p\right)_s/(\rho C_p)_f$

The relevant boundary conditions now becomes

u(z, t) = 0, v(z, t) = 0, T(z, t)=0, C(z, t)=0 for $t \le 0\ for\ any\ z$

u(0, t)=1+$\frac{\varepsilon}{2}(e^{int} + e^{-int})$, $v(0,t) = 0, T(0,t) = 1, C(0,t) = 1$

$u(\infty,t) \to 0, v(\infty,t) \to 0, T(\infty,t) \to 0, C(\infty,t) \to 0\ for\ t \ge 0$ (2.13)

Using eqn (2.9) the velocity characteristics U_0 is defined as:

$U_0 = \{g\beta_f(T_w - T_\infty)vf\}^{1/3}$

To obtain the desired solutions, we now simplify eqns (2.9-2.12) by putting the fluid velocity in the complex form as:

$U(z,t) = u(z,t) + iv(z,t)$ and we get

$A_3\left\{\frac{\partial U}{\partial t} - S\frac{\partial U}{\partial z} - iRU\right\} = \frac{1}{A_1}\frac{\partial^2 U}{\partial z^2} + A_4 T - \left(M + \frac{1}{K}\right)U$ (2.14)

The associated boundary conditions in eqn (3.3.13) becomes

U(z, t) = 0, T(z, t)=0, C(z, t)=0 for $t \le 0\ any\ z$

U(0, t)=1+$\frac{\varepsilon}{2}(e^{int} + e^{-int})$, $T(0,t) = 1, C(0,t) = 1$

$U(\infty,t) \to 0, v(\infty,t) \to 0, T(\infty,t) \to 0, C(\infty,t) \to 0\ for\ t \ge 0$ (2.15)

3.0 METHOD OF SOLUTIONS

To find the analytical solutions of the above system of partial differential equations (2.11), (2.12) and (2.14) subject to the boundary conditions (2.15) in the neighborhood of the plate, we assume that:

To solve the resultant nonlinear partial differential equations subject to the appropriate boundary condition, we will be using a regular perturbation technique. The unsteady flow is superimposed on the mean steady flow, so that in the neighborhood of the plate, we will assume the solutions of velocity, temperature and concentration to be as follows:

$U(z,t) = U_0(z,t) + \frac{\varepsilon}{2}\{e^{int}U_1\}$ (3.1)

$T(z,t) = T_0(z,t) + \frac{\varepsilon}{2}\{e^{int}T_1\}$ (3.2)

$C(z,t) = C_0(z,t) + \frac{\varepsilon}{2}\{e^{int}C_1\}$ (3.3)

Due to the nonlinearity of this resultant governing equations, we further make the following assumptions:

$\left.\begin{aligned} U_0(z,t) &= U_{00}(z,t) + Nt[U_{01}(z,t)] \\ U_1(z,t) &= U_{10}(z,t) + Nt[U_{11}(z,t)] \end{aligned}\right\}$ (3.4)

$\left.\begin{aligned} T_0(z,t) &= T_{00}(z,t) + Nt[T_{01}(z,t)] \\ T_1(z,t) &= T_{10}(z,t) + Nt[T_{11}(z,t)] \end{aligned}\right\}$ (3.5)

$\left.\begin{aligned} C_0(z,t) &= C_{00}(z,t) + Nt[C_{01}(z,t)] \\ C_1(z,t) &= C_{10}(z,t) + Nt[C_{11}(z,t)] \end{aligned}\right\}$ (3.6)

Substituting eqns (3.4-3.6) into eqns (3.1), (3.2) and (3.3), and comparing the coefficients of Nt^0 and Nt^1, after involving the above equations (3.1-3.3) into eqns (2.9-2.12) and equating the harmonic and non-harmonic terms and neglecting the higher order terms of $O(\varepsilon^2)$, we obtain the following set of equations:

The zeroth order equations are:

Velocity equations

$\frac{1}{A_1}\frac{\partial^2 U_{00}}{\partial z^2} + A_3 S\frac{\partial U_{00}}{\partial z} - \left(A_3 iR + M + \frac{1}{K}\right)U_{00} + A_4 T_{00} = 0$ (3.7)

$\frac{1}{A_1}\frac{\partial^2 U_{01}}{\partial z^2} + A_3 S\frac{\partial U_{01}}{\partial z} - \left(A_3 iR + M + \frac{1}{K}\right)U_{01} + A_4 T_{01} = 0$ (3.8)

DOI: https://doi.org/10.57233/ijsgs.v10i1.611 ISSNp: 2488-9229; ISSNe: 3027-1118

Temperature equations

$$A_2\frac{\partial^2 T_{00}}{\partial z^2}+A_5 SPr\frac{\partial T_{00}}{\partial z}-QT_{00}=0 \quad (3.9)$$

$$A_2\frac{\partial^2 T_{01}}{\partial z^2}+A_5 SPr\frac{\partial T_{01}}{\partial z}-QT_{01}=-Pr\left[\frac{\partial T_{00}}{\partial z}\right]^2 \quad (3.10)$$

Concentration equations

$$\frac{\partial^2 C_{00}}{\partial z^2}+SSc\frac{\partial C_{00}}{\partial z}-ScKrC_{00}=-ScSr\frac{\partial^2 T_{00}}{\partial z^2} \quad (3.11)$$

$$\frac{\partial^2 C_{01}}{\partial z^2}+SSc\frac{\partial C_{01}}{\partial z}-ScKrC_{01}=-ScSr\frac{\partial^2 T_{01}}{\partial z^2} \quad (3.12)$$

The first order equations are

Velocity equations

$$\frac{1}{A_1}\frac{\partial^2 U_{10}}{\partial z^2}+A_3 S\frac{\partial U_{10}}{\partial z}-\left(A_3 iR+M+\frac{1}{K}\right)U_{10}+A_4 T_{10}=0 \quad (3.13)$$

$$\frac{1}{A_1}\frac{\partial^2 U_{11}}{\partial z^2}+A_3 S\frac{\partial U_{11}}{\partial z}-\left(A_3 iR+M+\frac{1}{K}\right)U_{11}+A_4 T_{11}=0 \quad (3.14)$$

Temperature equations

$$A_2\frac{\partial^2 T_{10}}{\partial z^2}+A_5 SPr\frac{\partial T_{10}}{\partial z}-QT_{10}=0 \quad (3.15)$$

$$A_2\frac{\partial^2 T_{11}}{\partial z^2}+A_5 SPr\frac{\partial T_{11}}{\partial z}-QT_{11}=-Pr\left[\frac{\partial T_{10}}{\partial z}\right]^2 \quad (3.16)$$

Concentration equations

$$\frac{\partial^2 C_{10}}{\partial z^2}+SSc\frac{\partial C_{10}}{\partial z}-ScKrC_{10}=-ScSr\frac{\partial^2 T_{10}}{\partial z^2} \quad (3.17)$$

$$\frac{\partial^2 C_{11}}{\partial z^2}+SSc\frac{\partial C_{11}}{\partial z}-ScKrC_{11}=-ScSr\frac{\partial^2 T_{11}}{\partial z^2} \quad (3.18)$$

The corresponding boundary conditions can simply be written as:

$$U_{00}=U_{01}=U_{10}=U_{11}=1, T_{00}=T_{01}=T_{10}=T_{11}=1, C_{00}=C_{01}=C_{10}=C_{11}=1 \text{ at } z=0$$
$$U_{00}=U_{01}=U_{10}=U_{11}=0, T_{00}=T_{01}=T_{10}=T_{11}=0, C_{00}=C_{01}=C_{10}=C_{11}=0 \text{ at } z\to\infty\infty \quad (3.19)$$

Solving the above equations restricted to the boundary conditions (3.19), we obtain the expressions for velocity, temperature and concentration as:

$$T_{00}=e^{-c_2 z} \quad (3.20)$$

$$T_{01}=F_4 e^{-c_4 z}+F_5 e^{-2c_2 z} \quad (3.21)$$

$$T_{10}=e^{-c_6 z} \quad (3.22)$$

$$T_{11}=F_9 e^{-c_8 z}+F_{10} e^{-2c_6 z} \quad (3.23)$$

$$C_{00}=B_2 e^{-c_{10} z}+B_3 e^{-c_2 z} \quad (3.24)$$

$$C_{01}=B_5 e^{-c_{12} z}+B_6 e^{-c_4 z}+B_7 e^{-2c_2 z} \quad (3.25)$$

$$C_{10}=B_9 e^{-c_{14} z}+B_{10} e^{-c_6 z} \quad (3.26)$$

$$C_{11}=B_{12} e^{-c_{16} z}+B_{13} e^{-c_8 z}+B_{14} e^{-2c_6 z} \quad (3.27)$$

$$U_{00}=D_2 e^{-c_{18} z}+D_3 e^{-c_2 z} \quad (3.28)$$

$$U_{01}=D_5 e^{-c_{20} z}+D_6 e^{-c_4 z}+D_7 e^{-2c_2 z} \quad (3.29)$$

$$U_{10}=D_9 e^{-c_{20} z}+D_{10} e^{-c_6 z} \quad (3.30)$$

$$U_{11}=D_{12} e^{-c_{22} z}+D_{13} e^{-2c_6 z} \quad (3.31)$$

Recall that

$$\left.\begin{aligned}U_0(z,t)&=U_{00}+Nt[U_{01}]\\U_1(z,t)&=U_{10}+Nt[U_{11}]\end{aligned}\right\} \quad \textbf{(3.32)}$$

$$\left.\begin{aligned}T_0(z,t)&=T_{00}+Nt[T_{01}]\\T_1(z,t)&=T_{10}+Nt[T_{11}]\end{aligned}\right\} \quad \textbf{(3.33)}$$

$$\left.\begin{aligned}C_0(z,t)&=C_{00}+Nt[C_{01}]\\C_1(z,t)&=C_{10}+Nt[C_{11}]\end{aligned}\right\} \quad (3.34)$$

$$U(z,t)=U_0+\frac{\varepsilon}{2}\{e^{int}U_1\} \quad (3.35)$$

$$T(z,t)=T_0+\frac{\varepsilon}{2}\{e^{int}T_1\} \quad (3.36)$$

$$C(z,t)=C_0+\frac{\varepsilon}{2}\{e^{int}C_1\} \quad (3.37)$$

The physical quantities of engineering interest are skin friction, Nusselt number and Sherwood number coefficients, which have been derived as follows:

$$\left.\frac{dU}{dz}\right|_{z=0}=-c_{18}D_2-c_2D_3+Nt(-c_{20}D_5-c_4D_6-2c_2D_7)+\frac{\varepsilon}{2}[-c_{20}D_9-c_6D_{10}+Nt(-c_{22}D_{12}-c_4D_6-2c_6D_{13})]e^{int} \quad (3.38)$$

$$\left.\frac{dT}{dz}\right|_{z=0}=-c_2+Nt(-c_4F_4-c_2F_5)+\frac{\varepsilon}{2}[-c_6+Nt(-c_8F_9-2c_6F_{10})]e^{int} \quad (3.39)$$

$$\left.\frac{dC}{dz}\right|_{z=0}=-c_{10}B_2-c_2B_3+Nt(-c_{12}B_5-c_4B_6-2c_2B_7)+\frac{\varepsilon}{2}[-c_{14}B_9-c_6B_{10}+Nt(-c_{16}B_{12}-c_8B_{13}-2c_6B_{14})]e^{int} \quad (3.40)$$

4.0 RESULTS AND DISCUSSION

In order to get physical insight into the problem, we have carried out numerical calculations for non-dimensional velocity, temperature and species concentration, skin-friction, and Nusselt number by assigning some specific values to the parameters entering into the problem for basically three different types of water based nanofluids. For this purpose, Figs. 4.2-4.11 have been plotted and discussed. Table 1 shows the thermo physical properties of water and the Nano elements Cu, Al_2O_3 and TiO_2. To ascertain the validity and correctness of this present investigation,

DOI: https://doi.org/10.57233/ijsgs.v10i1.611 ISSNp: 2488-9229; ISSNe: 3027-1118

IJSGS FUGUSAU VOL10 (1) WEBSITE: https://fugus-

the graphs for temperature and velocity profiles as shown in Figs 4.1a and b for Narayana and Venkateswarlu (2016) and the current study for limiting case when $Nt \rightarrow 0$ for fixed values of ε =0.01; R=0.02 n=10.0; t=0.1; M=0.5, K=S=Kr=1; Q=10.0: $\emptyset = 0.15$.

Table 1: Thermo-Physical Properties

Physical properties	Water	Copper (Cu)	Aluminium Oxide (Al_2O_2)	Titanium oxide (TiO_2)
C_p	4179	385	765	686.2
ρ	997.1	8933	3970	4250
K	0.613	400	40	8.9538
$\beta \times 10^{-5}$	21	1.67	0.85	0.9

The comparison demonstrates an excellent relationship. Figures 4.2 and 4.3 present the effects of the thermophoresis parameter Nt on the temperature distribution and nanoparticle concentration. With an increase in Nt, the temperature of the fluid increases. Equally, an increase in Nt results to an increase in the nanoparticle concentration. From the physical point of view, an increase in Nt results to an increase in the thermophoresis force which tends to move nanoparticles form the hot to cold region consequently increasing the magnitude of the temperature profiles and the nanoparticle concentration profiles. An increase in the thermophoresis parameter results to thickening of the nanoparticles concentration boundary layer. The deviations of temperature profiles for different values of heat sink parameter Q is sketched in Figure 4.4. It is clear that, there is a decrease in the temperature with increase of Q. This is due to the fact that when heat is absorbed, the buoyancy forces decrease which retard the flow rate and thereby give rise to a decrease in the temperature profile. The variations of Darcy porous parameter on the velocity gradient is illustrated in Figure. 4.5. Figure 4.6 depicts the action of the Darcy porosity parameter on the velocity nanoparticles gradient. It is perceived from this figure that the velocity fluid accelerates as the porosity parameter is increased. We observe that, with the growth in permeability of the porous medium, the drag force weakens; because of this, velocity gradient of the fluid blows up. Moreover, this makes sense because when a lot of fluid is moved, more viscous energy is made. This causes the fluid boundary wall and thickness to grow, which speeds up the movement of the fluid. Figure 4.7 shows the influence of magnetic field parameter M on the velocity Nanofluid profiles in the boundary layer. Application of magnetic field to an electrically conducting fluid gives rise to a resistive type force called the Lorentz force. This force has the tendency to slow down the motion of the fluid in the boundary layer. Thus the presence of the magnetic field parameter decreases the momentum boundary layers' thickness. Figure 4.8 shows the effect of chemical reaction (Kr) on concentration profile. Its observed that increase in chemical reaction parameter decreases the concentration profile. The rationale is that as chemical reactions increases, the quantity of solute molecules undergoing them grows, this causes concentration to drop, which in turn reduces the likely-hood of destructive chemical reaction. In other words, the concentration asymptotically decreases from the maximum value 1 to 0 as z →∞. This shows that the concentration field is greatest near the plate surface and least in the outer flow region. The same figure further indicates that there is a steady fall in species concentration due to the effect of chemical reaction. This means that the consumption of chemical species leads to fall in the species concentration field. This clearly agrees with the physical laws. Figure 4.9 demonstrates how the species concentration rises along with the number of Sorets. A rise in the Soret effect, by definition, indicates an increase in molar mass diffusivity. An increase in the increase in concentration is due to molecule mass diffusivity. This shows that the species concentration in the fluid tends to rise as the Soret number rises. The deviations of magnetic number versus suction/injection parameters on the skin friction is displayed in Figure 4.10. it is evident that increasing the magnetic and suction/injection effects strengthens the skin friction and this effect is higher in the case of Cu-water nano element than Ai_2O_3 and TiO_2 nano elements. The impacts of Nt on the rates of heat and mass transfer are exhibited in The coefficients of Nusselt number and Sherwood number are plotted against Q and Sr respectively for different values of Nt in Figs. 4.11 and 4.12. It is obvious that the rates of heat and mass transfers increase with rising values of Nt. It is also observed that Cu -water nanofluid has the highest Nusselt number.

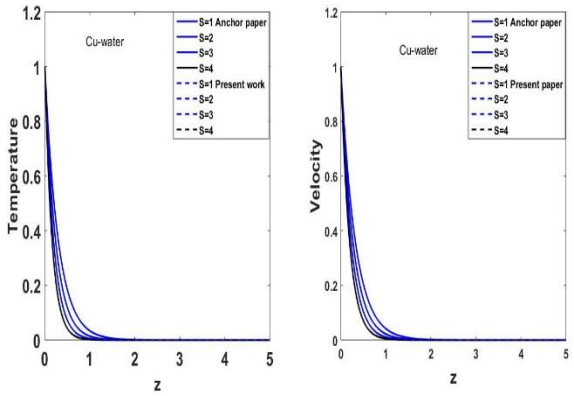

Figure 4.1 Comparison of Narayana and Venkateswarlu 2016 with the present work for (a) temperature and (b) velocity gradient

DOI: https://doi.org/10.57233/ijsgs.v10i1.611 ISSNp: 2488-9229; ISSNe: 3027-1118

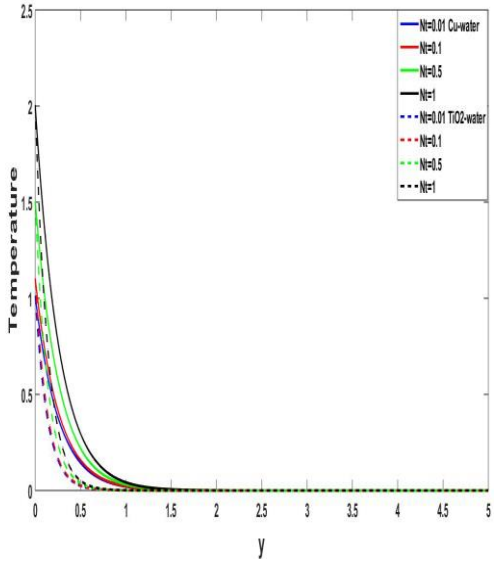

Figure 4.2 Action of Nt on temperature gradient

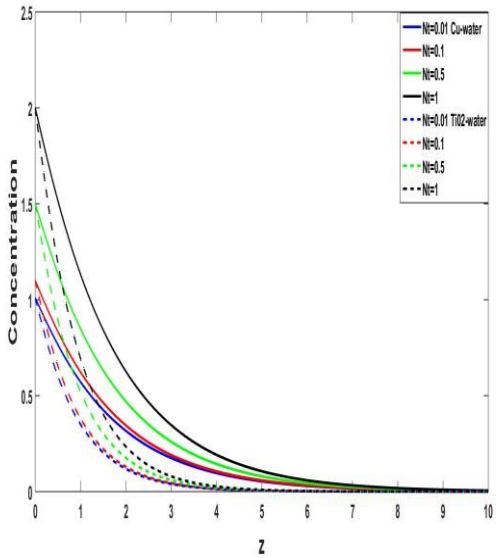

Figure 4.3 Action of Nt on concentration gradient

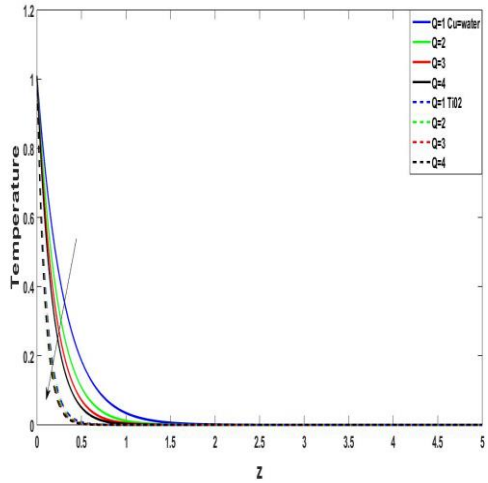

Figure 4.4 Action of Q on temperature gradient

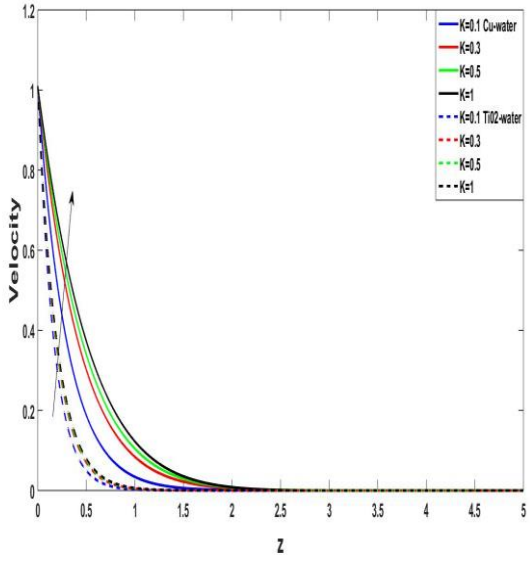

Figure 4.6 Action of K on velocity gradient

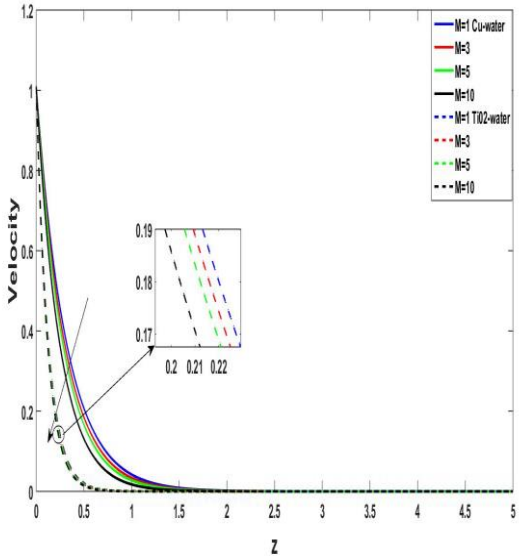

Figure 4.7 Action of M on velocity gradient

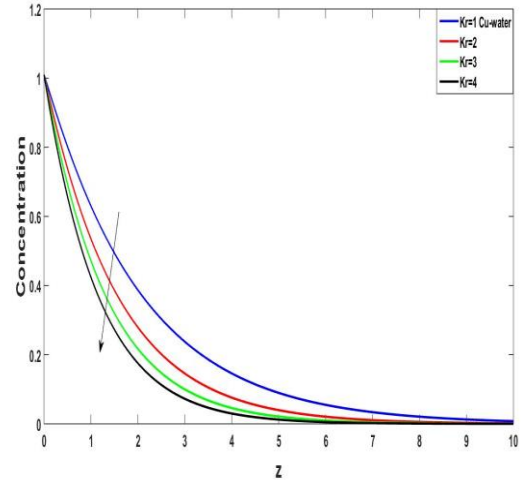

Figure 4.8 Action of Kr on concentration gradient

DOI: https://doi.org/10.57233/ijsgs.v10i1.611 ISSNp: 2488-9229; ISSNe: 3027-1118

IJSGS FUGUSAU VOL10 (1) WEBSITE: https://fugus-

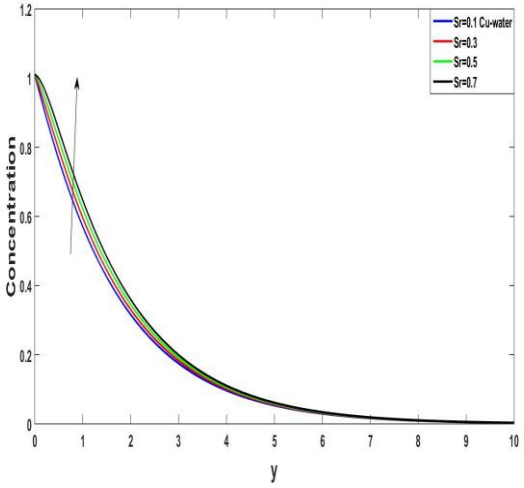

Figure 4.9 Action of Sr on concentration gradient

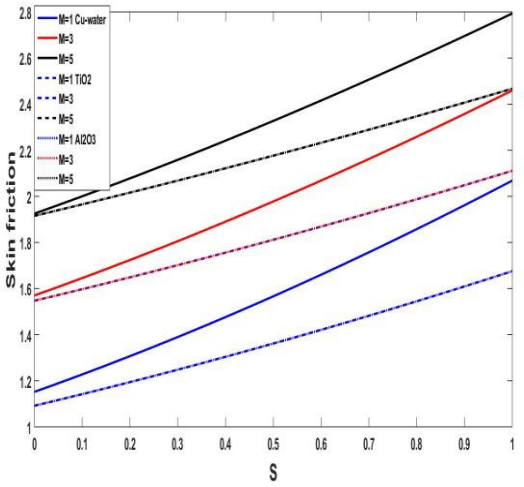

Figure 4.10 Action of M against S on skin friction

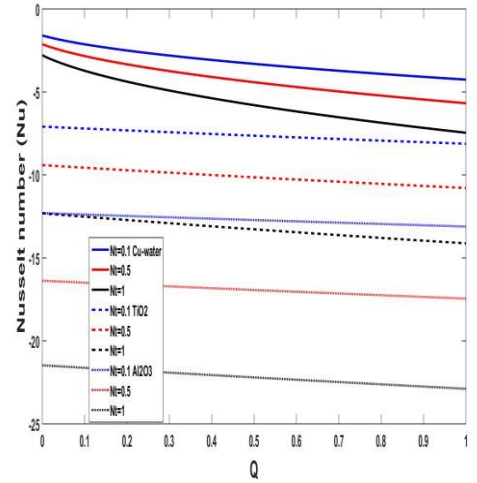

Figure 4.11 Action of Nt against Q on Nusselt number

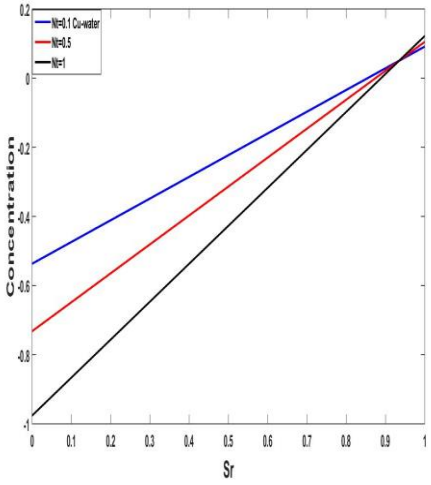

Figure 4.12 Action of Nt against Sr on Sherwood number

5.0 CONCLUSION

The effects of Thermophoresis parameter variation on heat and mass transfer on MHD oscillatory nanofluid flow in a permeable plate equipped with porous material was considered and researched. The nanofluid velocity, temperature and concentration profiles have been calculated for pertinent controlling parameters on the flow configuration. The physical components of engineering interest have also been computed such as nanofluid skin friction, Nusselt number and Sherwood number. We hope that the findings of this investigation may be useful in catalysis, biomedicine, magnetic resonance imaging, data storage and environmental remediation. Hence, the subject of nanofluids is of great interest worldwide for basic and applied research. The summary of the noteworthy findings is given below:

i. It is seen that increasing the Thermophoresis parameter Nt leads to an increase in heat transfer and a decrease in mass transfer. Additionally, thermophoresis Nt have a significant impact on the MHD flow, and can be used to control the heat and mass transfer rates in MHD fluid flow by altering the parameters to achieve expected flow velocity that gives the required heat and mass transfer in an engineering process.

ii. The copper nanoparticles proved to have the maximum cooling recital for this vertical porous plate problem where Alumina nanoparticles have the lowest. This is due to the high thermal conductivity of Cu and low thermal conductivity of Al_2O_3 and TiO_2

iii. The velocity profile decreases with an increase in nanoparticle magnetic parameter, while the opposite is true when the Darcy porous parameter is increased.

iv. Due to chemical reaction, the concentration of the fluid decreases. This is because the consumption of chemical species leads to a fall in the species concentration field. This remarkable feature of the concentration profiles in our

investigation is due to the presence of Soret number and nanoparticles in the flow field.

v. It has been shown that mixing nanoparticles in a liquid (nanofluid) has a dramatic effect on the liquid thermophysical properties such as thermal conductivity.

REFERENCES

Abbas, M. A., Ahmed, B., Li, C., Rehman, S. U., Saleem, M. and Khudair, W. S. (2022). Analysis of entropy generation on magnetohydrodynamic flow with mixed convection through porous media, Energies, 15 (3), 1206, https://doi.org/10.3390/en15031206.

Ajibade A. O., Gambo J. J. and Jha B. K. (2023). Effects of viscous and Darcy dissipation on fully developed natural convection flow in a composite channel partially filled with porous material: Homotopy perturbation method (HPM), Journal of Applied Mathematics and Mechanics, 103(6), https//doi.org/10.1002/zamm.202100583

Alam Md. Shariful (2016). Effect of Thermophoresis on MHD Free Convective Heat and Mass Transfer Flow along an Inclined Stretching Sheet under the Influence of Dufour-Soret Effects with Variable Wall Temperature, Thammasat International Journal of Science and Technology, 21(3), pp 48-58.

Alam N., Poddar S., Karim M. E, Hasan M. S. and Lorenzini G. (2021). Transient MHD radiative fluid flow over an inclined porous plate with thermal and mass diffusion: an EFDM numerical approach. International Information of Engineering and Technological Associations, 8(5), pp. 739-749.

Alvarez, M., Colmenares, E. and Sequeira, F. A. (2022). Analysis of a semi-augmented mixed finite element method for double-diffusive natural convection in porous media, Computational Mathematics and Applications, 114, pp. 112–131, https://doi.org/10.1016/j.camwa.2022.03.032.

Bordoloi R., Chamuah K. and Ahmed N. (2023). Free Convective MHD Radiative Flow Past a Porous Vertical Plate in a Porous Medium with Chemical Reaction, Biointerface Research in Applied Chemistry, 13 (3), pp. 1-15.

Chamkha, A. J., Aly, A. M. and Al-Mudhaf, H. (2011). Laminar MHD mixed convection flow of a nanofluid along a stretching permeable surface in the presence of heat generation or absorption effects. International Journal of Microscale, Nanoscale and Thermal Fluid Transfer Phenomena 2(1), pp. 51–70.

Chitra M. and Suhasini M. (2018). Effect of unsteady oscillatory MHD flow through a porous medium in porous vertical channel with chemical reaction and concentration, National Conference on Mathematical Techniques and its Applications, 012039, doi :10.1088/1742-6596/1000/1/012039

Choi, S.U. and Eastman, J.A. (1995). Enhancing thermal conductivity of fluids with nanoparticles. (No. ANL/MSD/CP-84938: CONF-951135-29.

Chu Y., Aziz S., Ijaz K. M., Khan S. U., Nazeer M., Ahmad I. and Tlili, I. (2020). Nonlinear radiative bioconvection flow of Maxwell nanofluid configured by bidirectional oscillatory moving surface with heat generation phenomenon, Physica Scriptavol 95(10). https://doi.org/10.1088/1402-4896/abb7a9

Gambo D., Yusuf, T. S., Oluwagbemiga, S. A., Kozah, J. D. and Gambo J. J. (2021). Analysis of free convective hydromagnetic flow of heat generating/absorbing fluid in an annulus with isothermal and adiabatic boundaries. Partial Differential Equations in Applied Mathematics. https://doi.org/10.1016/j.padiff.2021.100080

Gambo J. and Gambo D. (2020). On the effect of heat generation/absorption on magneto-hydrodynamic free convective flow in a vertical annulus: An Adomian decomposition method. Heat transfer, Wiley. 50(1), 1-15.DOI: 10.1002/hti.21978.

Gbadeyan, J. A., Titiloye, E.O., and Adeosun, A. T. (2020). Effect of variable thermal conductivity and viscosity on Casson nanoflui9d flow with convective heating and velocity slip. Heliyon, 6(1), e03076.

Gireesha B. J. and S. Sindhu, (2020). MHD natural convection flow of casson fluid in an annular microchannel containing porous medium with heat generation/absorption. Nonlinear Engineering, 9, pp. 23-232.

Hasan, N. Z. Mohammed, Y. Nasreen, S. N. (2020). Effects of thermal radiation, heat generation and induced Magnetic field on Hydromagnetic free convective flow of couple stress fliud in an isoflux-isothermal vertical channel, Journal of Applied Mathematics, vol.2020, Article ID 4539531.

Jalili P., Azar A. A., Jalili B. and Ganji D. D. (2023). A novel technique for solving unsteady three-dimensional brownian motion of a thin film nanofluid flow over a rotating surface, Scientific Reports, 13,13241 | https://doi.org/10.1038/s41598-023-40410-3

Jha B. K. and Samaila G. (2022). MHD natural convection heat and mass transfer flow over an inclined porous plate with thermophoresis and nonlinear thermal radiation effects, Heat Transfer, 52(3), pp. 2490-2513.

Kadeethum, T., Ballarin, F., Choi, Y., O'Malley, D., Yoon, H and Bouklas, N. (2022). Non-intrusive reduced order modeling of natural convection in porous media using convolutional autoencoders: comparison with linear subspace techniques, Advances in Water Resources, 160, 104098.

Khalil, W. H., Azzawi, I. D. J. and Damook, A. A. (2022). The optimization of MHD free convection inside porous trapezoidal cavity with the wavy bottom wall using response surface method, International Communications in Heat and Mass Transfer, 134, 106035, https://doi.org/10.1016/j.icheatmasstransfer.2022.106035.

Khedher, N. B., Ullah, Z., Mahrous, Y. M., Dhahbi, S., Ahmad, S., Abu-Zinadah, H., & Faqihi, A. A. (2024). Viscous dissipation effect on amplitude and oscillating frequency of heat transfer and electromagnetic waves of magnetic driven fluid flow along the horizontal circular cylinder. Case Studies in Thermal Engineering, 55. https://doi.org/10.1016/j.csite.2024.104142

Khan, W. A. and Pop, I. (2010). Boundary-layer flow of a nanofluid past a stretching sheet. International Journal of Heat and Mass Transfer 53(11), 2477–2483.

Mabood, F., and Usman, H. (2019). Multiple slip effects on MHD thermo-solutal flow in porous media saturated by nanofluid. Mathematical modelling of engineering problems, 6(4), 502-510.

Narayana P.V. S. and Venkateswarlu B. (2016). Heat and mass transfer on mhd nanofluid flow past a vertical porous plate in a rotating system, Frontiers in Heat and Mass Transfer, 7(8), DOI: 10.5098/hmt.7.8

Ojemeri G. and Onwubuya I. O. (2023). Analysis of mixed convection flow on Arrhenius-controlled heat generating/absorbing fluid in a superhydrophobic microchannel: A semi-analytical approach, Dutse Journal of Pure and Applied Sciences, 9, 344-357.

Ojemeri, G. and Hamza, M. M. (2022). Heat transfer analysis of Arrhenius-controlled free convective hydromagnetic flow with heat generation/absorption effect in a micro-channel, Alexandria Engineering Journal, 61, pp. 12797-12811.

Ojemeri, G., Onwubuya I. O., Omokhuale, E., Hussaini A. and Shuaibu, A. (2024). Analytical investigation of Arrhenius kinetics with heat source/sink impacts along a heated superhydrophobic microchannel, UMYU Scientifica, 3(1), 61-71.

Oni M. O. and Jha B. K. (2019). Heat generation/absorption effect on natural convection flow in a vertical annulus with time-periodic boundary conditions. Journal of Aircraft and Spacecraft technology, 3(1), 183-196. https://doi.org/10.3844/jastsp.2019.183.196

Parthiban S. and Prasad V. R. (2023). Thermal radiation and Hall current effects in a MHD non-Darcy flow in a differentially heated square enclosure Lattice-Boltzmann simulation. Journal of porous media, Begell house, 26(5), pp37-56.

Salah F., Sidahmed A. O. M. and Viswanathan K. K. (2023). Chemical MHD Hiemenz flow over a nonlinear stretching sheet and Brownian motion effects of nanoparticles through a porous medium with radiation effect, Mathematical Computer and Modeling of Fluid Flow and Heat Transfer, 28(1), 21, DOI: 10.3390/mca28010021

Saleem, S., Nazeer, M., Radwan, N., & Abutuqayqah, H. (2024). Significance of hafnium nanoparticles in hydromagnetic non-Newtonian fluid-particle suspension model through divergent channel with uniform heat source: thermal analysis. Zeitschrift für Naturforschung A, (0). https://doi.org/10.1515/zna-2023-0336

Sharma B. K., Khanduri U., Mishra N. K. and Mekheimer Kh. S (2023). Combined effect of thermophoresis and Brownian motion on MHD mixed convective flow over an inclined stretching surface with radiation and chemical reaction, International Journal of Modern Physics B, 37(10), 2350095.

Sharma T., Sharma P. and Kumar N. (2022). Study of dissipative MHD oscillatory unsteady free convective flow in a vertical channel occupied with the porous material in the presence of heat source effect and thermal radiation, International Symposium on Fluids and Thermal Engineering, 012012. doi:10.1088/1742-6596/2178/1/012012.

Suma U. K., Katun M. and Biswas R. (2023). Consequences of Thermophoresis, and Brownian Motion on MHD Heat and Mass Transfer of Jeffrey's Nano-fluid Flow Via a Perpendicular Plate, Asian Journal of Pure and Applied Mathematics, 5(1), 414-429,

Suma U. K., Katun M. and Biswas R. (2023). Consequences of Thermophoresis, and Brownian Motion on MHD Heat and Mass Transfer of Jeffrey's Nano-fluid Flow Via a Perpendicular Plate, Asian Journal of Pure and Applied Mathematics, 5(1), 414-429,

Usman and Sanusi (2023). Heat and mass transfer analysis for the mhd flow of Casson nanofluid in the presence of thermal radiation, FUDMA Journal of Sciences, 7(2), pp 188 – 198.

Usman H. and Sanusi S. (2023). Heat and mass transfer analysis for the mhd flow of Casson nanofluid in the presence of thermal radiation, FUDMA Journal of Sciences, 7(2), pp 188 – 198.

Waini I., Hamzah K. B., Khashi'ie N. S., Zainal N. A., Kasim A. M., Ishak A., Ioan Pop I. (2023). Brownian and thermophoresis diffusion effects on magnetohydrodynamic Reiner–Philippoff nanofluid flow past a shrinking sheet, Alexandria Engineering Journal, 67, pp. 183-192.

Zhao T., Khan M. and Chu Y. (2020) Artificial neural networking (ANN) analysis for heat and entropy generation in flow of non-Newtonian fluid between two rotating disks, Math. Method Applied Sci, https://doi.org/10.1002/mma.7310

Appendix

DOI: https://doi.org/10.57233/ijsgs.v10i1.611 ISSNp: 2488-9229; ISSNe: 3027-1118

IJSGS FUGUSAU VOL10 (1) WEBSITE: https://fugus-

$c_1 = c_3 = c_5 = c_7 = \frac{-A_5SPr+\sqrt{(A_5SPr)^2+4A_2Q}}{2A_2}$, $c_2 = c_4 = c_6 = c_8 = \frac{A_5SPr+\sqrt{(A_5SPr)^2+4A_2Q}}{2A_2}$,

$c_9 = c_{11} = c_{13} = c_{15} = \frac{-SSc+\sqrt{(SSc)^2+4ScKr}}{2}$, $c_{10} = c_{12} = c_{14} = c_{16} = \frac{SSc+\sqrt{(SSc)^2+4ScKr}}{2}$,

$c_{17} = c_{19} = c_{21} = c_{23} = \frac{-A_1A_3S+\sqrt{(A_1A_3S)^2+4A_1w_2}}{2}$, $c_{18} = c_{20} = c_{22} = c_{24} = \frac{A_1A_3S+\sqrt{(A_1A_3S)^2+4A_1w_2}}{2}$, $w_2 = A_3iR + M + \frac{1}{K}$, $F_5 = \frac{-Prc_2^2}{4A_2c_2^2-2A_5SPrc_2-Q}$, $F_9 = 1 - F_5$

$F_{10} = \frac{-Prc_6^2}{4A_2c_6^2-2A_5SPrc_6-Q}$, $F_9 = 1 - F_{10}, B_3 = \frac{-ScSrc_2^2}{4c_2^2-SScc_2-ScKr}$, $B_2 = 1 - B_3, B_6 = \frac{-ScSrc_4^2F_4}{c_4^2-SScc_4-ScKr}, B_7 = \frac{-4ScSrc_2^2F_5}{4c_2^2-2SScc_2-ScKr}, B_5 = 1 - B_6 - B_7$, $B_9 = 1 - B_{10}, B_{10} = \frac{-ScSrc_6^2}{c_6^2-SScc_6-ScKr}, B_{13} = \frac{-ScSrc_8^2F_9}{c_8^2-SScc_8-ScKr}$,

$B_{14} = \frac{-4ScSrc_6^2F_{10}}{4c_6^2-2SScc_6-ScKr}, B_{12} = 1 - B_{13} - B_{14}$, $D_3 = \frac{-A_4}{\frac{c_2^2}{A_1}-A_3Sc_2-w_2}, D_2 = 1 - D_3$, $D_6 = \frac{-A_4F_4}{\frac{c_4^2}{A_1}-A_3Sc_4-w_2}$, $D_7 = \frac{-A_4F_5}{\frac{c_2^2}{A_1}-A_3Sc_2-w_2}$, $D_5 = 1 - D_6 + D_7$, $D_{10} = \frac{-A_4}{\frac{c_6^2}{A_1}-A_3Sc_6-w_2}$, $D_9 = 1 - D_{10}$, $D_{13} = \frac{-A_4}{4\frac{c_6^2}{A_1}-2A_3Sc_6-w_2}$, $D_{12} = 1 - D_{13}$,

NOMENCLATURE

B_0	constant applied magnetic field
τ	skin friction coefficient
C_p	specific heat at constant pressure
C_∞	concentration of the solute far away from the plate
D_m	molecular diffusivity
E	applied electric field
g	acceleration due to gravity
K	permeability parameter
k	permeability of porous medium
k∗	mean absorption coefficient
M	dimensionless magnetic field parameter
Nu	Nusselt number
Pr	Prandtl number
Nt	Thermophoresis parameter
Q	dimensional heat sink parameter
R	dimensional rotational parameter
Kr	chemical reaction parameter
S	suction parameter
Sc	Schmidt number
Sr	Soret number
Sh	Sherwood number
w	condition at the wall
T	local Temperature of the nanofluid
T_w	wall temperature of the fluid
T_∞	temperature of the ambient nanofluid
U_0	characteristic velocity
(u,v,w)	velocity components along x and y axes

GREEK SYMBOLS

α	thermal diffusivity
α_f	thermal diffusivity of the fluid
α_{nf}	thermal diffusivity of the nanofluid
β	thermal expansion coefficient
β_f	coefficient of thermal expansion of the fluid
β_s	coefficient of thermal expansion of the solid
$(\rho C_p)_{nf}$	heat capacitance of the nanofluid
σ ∗	Stefan-Boltzmann constant parameter
σ	electrical conductivity of the fluid
ρ_f	density of the fluid friction
ρ_{nf}	density of the nanofluid
ρ_s	density of the solid friction
ν_f	kinematic viscosity of the fluid
ν	kinematic viscosity
μ_{nf}	viscosity of the nanofluid
μ	dynamic viscosity
ε	small constant quantity
U	complex velocity
T	non-dimensional Temperature
C	non-dimensional Concentration

SUBSCRIPT

f	fluid
s	solid
n_f	nanofluid
∞	condition at free stream